

Research on Vehicle Scheduling of Battery Swap Stations Based on Online Information Platforms

Chengze Li¹, Junxiang Li^{1,2*}, Ziyi Yang¹

¹Business School, University of Shanghai for Science & Technology, Shanghai 200093, China

²School of Intelligence Emergency Management, University of Shanghai for Science & Technology, Shanghai 200093, China

*Corresponding author, lijx@usst.edu.cn

Abstract: *To improve the emergency power supply capability of power grids under sudden blackouts, a hierarchical response scheduling model for a "battery swap station energy hub" is constructed relying on an online information platform and on the premise that battery swap stations are extensively deployed in residential communities. The first-level response is directly triggered by a power grid blackout signal, where the battery swap station acts as an energy storage device to provide emergency power directly to the community power grid. The second-level response relies on the online information platform: when the remaining power of the battery swap station falls below a preset threshold, nearby electric vehicle users are scheduled via various enterprise online platforms to intelligently replenish the battery swap station's power, ensuring a continuous power supply to the community. For the second-level response, based on real-time online data of battery swap stations, the scope and quantity of user notifications are determined, and a threshold model for users' safe return power is established. Combined with online vehicle location information and real-time traffic data, a dual-scheme scheduling strategy of time priority and distance priority is proposed, and battery swap information is accurately pushed to target vehicles through online information channels. An online simulation scenario is constructed based on the road network informatization characteristics of Shanghai, and comparative experiments are conducted. The results show that the proposed online scheduling model can stabilize the power of battery swap stations near the low threshold and gradually increase it to the target high value, significantly improving the continuity and stability of emergency power supply. It provides theoretical support and engineering reference for the intelligent scheduling of emergency resources of automotive battery swap stations relying on online information platforms and enhancing the emergency resilience of power grids.*

Keywords: Vehicle battery swap station, Emergency power supply, Online platform, Virtual road network, Intelligent scheduling, Power grid resilience.

1. Introduction

With the rapid development and popularization of the electric vehicle industry, practical contradictions such as insufficient supply of charging facilities and non-standard charging equipment in residential communities have become increasingly prominent, severely restricting the promotion and application of electric vehicles. As mentioned in Reference [1], against this background, the battery swapping mode has gradually emerged as a new trend to address industry pain points and lead the transformation of the energy replenishment system for new energy vehicles, owing to its efficient and convenient energy supplement advantages. On the premise that battery swap stations are extensively deployed in communities, the deep integration of information platforms and vehicle scheduling provides core support for the intelligentization and online operation of the battery swapping mode. In emergency situations such as sudden community power outages, battery swap stations can directly supply power to residents through on-site batteries. When the power grid fails to recover for a long time, online real-time monitoring of the emergency power supply status is realized via information platforms, enabling accurate scheduling of nearby electric vehicles and guiding them to swap batteries at the stations to replenish energy. This effectively extends the duration of emergency power supply and minimizes risks to residents' lives and property caused by power outages.

Domestic and foreign scholars have conducted extensive research on related issues. In terms of electric vehicle information platform technologies, Reference [2] studied an intelligent vehicle information management system based on the Internet of Things. By integrating advanced sensors, communication technologies, and data analysis methods, the

system meets the requirements of real-time monitoring, intelligent decision-making, and security. The results show that the system maintains stable performance under high load, effectively improves traffic safety and operational efficiency, and promotes the development of intelligent transportation. Reference [3] investigated the business model and development of the electric vehicle charging industry, proposing three stages of charging platform business models. In the third stage, an operational framework of an e-commerce platform for smart charging with information sharing was constructed, and its participants, operation process, carbon reduction benefits, and limitations were analyzed, providing insights for the development of the electric vehicle industry. Reference [4] reviewed the current status of testing and application of information security for intelligent connected vehicles from the perspectives of information security risks, research progress of domestic and international information security standards, and information security testing, offering a reference for related testing work. Reference [5] proposed an online monitoring and early warning method for the state of health of electric vehicle batteries, with data transmitted to a vehicle monitoring platform in real time via wireless communication, providing strong support for battery fault diagnosis and early warning. Reference [6] designed a low-cost, low-power online monitor for the joint estimation of lithium battery state of charge (SOC) and state of health (SOH), offering technical reference for the application and promotion of lithium batteries. Reference [7] introduced a novel hybrid model CART-GX that integrates advanced deep learning techniques to improve SOH prediction. Reference [8] explored the potential of digital twin (DT) technology to enhance traditional battery management systems (BMS) through intelligent and adaptive control.

Regarding vehicle scheduling, Reference [9] proposed an integrated “battery-vehicle matching” scheduling strategy to tackle problems such as additional battery life degradation and large variations in driving range for electric buses in cold regions under extreme temperature differences, helping bus operators formulate better operation plans. Reference [10] focused on emergency vehicle rescue scheduling on urban expressway networks. Centering on the optimal siting of emergency rescue resources and intelligent scheduling of rescue vehicles, an intelligent management model for emergency resources in complex traffic environments was developed to enhance the resilience of urban traffic networks. Reference [11] investigated vehicle scheduling management in a traditional Chinese medicine hospital, exploring the technical application of automated and visualized vehicle scheduling based on software platforms. Reference [12] presented real-time vehicle scheduling strategies in multimodal transport, which employ a two-step ride-matching algorithm to reduce traveler waiting time. Reference [13] proposed an electric vehicle charging scheduling strategy considering user willingness and status quo bias, improving user charging satisfaction, optimizing power grid load dispatch, and reducing operation costs. Reference [14] quantified the functional attributes of supply and demand parties according to the resource organization characteristics in shared manufacturing, and constructed a distributed flexible service resource scheduling model for shared manufacturing considering supply-demand matching, with the objectives of minimizing the maximum completion time and total cost.

2. Model Establishment

2.1 Emergency Response Mechanism

First-Level Response Triggering

When a sudden power outage occurs in a residential community, the first-level response is triggered. The community battery swap station acts as an energy storage device, and the stations within the blackout area directly supply power from their on-site batteries to residents in an emergency.

Second-Level Response Triggering

If the power outage persists for an extended period, the second-level response can be activated. The activation conditions are that the remaining power of the battery swap station falls below the preset minimum alarm threshold of its total capacity, and the grid power has not been restored. During the second-level response, the battery swap station will function as a battery swapping hub. Relying on an online information push platform, battery swapping information is sent to electric vehicle users to dispatch eligible vehicles to exchange batteries at the station, thereby replenishing energy for the swap station and extending the duration of emergency power supply.

2.2 Basic Assumptions for Energy Scheduling in the Second-Level Response

To simplify the computational complexity of online scheduling, the following basic assumptions are made: Electric vehicles travel at a constant speed to avoid

complicated energy consumption calculations involving acceleration and deceleration. Battery energy consumption is only related to travel distance, ignoring disturbances such as air conditioning and road gradient. Only single-path optimization from the starting point to the battery swap station is considered, without involving multi-station endurance chains. All candidate paths are of the same road type (e.g., all urban roads or expressways) to avoid excessive differences in energy consumption and speed. For calculation convenience, the power consumption of battery swapping at the station is neglected. According to the technical whitepaper (public operation and maintenance data) of a certain brand of battery swap stations, the power consumed by a single battery swap by the robotic arm is approximately 0.1 kWh–0.3 kWh, which is negligible compared with the rated battery capacity of 100 kWh.

2.3 Push Range Model

When the battery swap station initiates the second-level response, its online scheduling system sends an emergency battery swap request to users within the effective push range, and provides information on the remaining return-trip power after battery replacement, allowing users to decide whether to provide support. For users willing to support battery swapping, a reasonable push range must first be determined. Users who are too far away cannot meet the objective conditions even if they are willing, as their remaining power upon arrival at the swap station will not satisfy the station’s energy demand. Therefore, ineffective push notifications should be avoided. Under ideal conditions, the maximum push distance for a fully charged electric vehicle is:

$$S_2 = \frac{(Q_e - Q_f)}{W_3} \quad (1)$$

$$Q_f = \theta_4 + \theta_5 \quad (2)$$

$$\theta_4 \geq \frac{W_4}{N_t} \quad (3)$$

In Equation (1), S_2 denotes the maximum push distance under ideal conditions, Q_e is the rated capacity of the battery, kQ_e represents the minimum capacity to be retained in the swapped battery, and W_3 is the power consumption per 100 kilometers. In Equation (2), the minimum required power of the replaceable battery Q_f consists of two parts: θ_4 is the minimum power that the battery needs to provide to the swap station, and θ_5 is the user’s safe return power. In Equation (3), N_t is the maximum hourly capacity of the battery swap station, corresponding to the maximum number of battery swaps, the number of vehicles to be pushed. W_4 is the hourly emergency power demand of residents supplied by the swap station. To reduce the risk of failing to meet the power supply demand, θ_4 shall not be lower than the average emergency demand allocated to vehicles in each round of push.

2.4 Mathematical Model of User Safe Return Power

The determination of the user’s safe return power θ_5 in Equation (2) is crucial, as it exerts a significant and mutually constraining influence on the user set size S and the user consent rate P_1 . An increase in θ_5 raises the minimum required power Q_f of replaceable batteries, which reduces the number of vehicles meeting the power requirement and

shrinks the user set. However, a higher safe return power better satisfies the return travel demand of users after battery swapping, thereby improving the user consent rate. Conversely, a decrease in θ_5 lowers the minimum required power Q_f , expanding the user set that satisfies the battery power condition, but reduces the user consent rate due to insufficient safe return power. Therefore, accurately determining the value of θ_5 to maximize the number of consenting users is of great theoretical and practical significance for improving energy scheduling efficiency and optimizing resource allocation. Let the user set within the effective push range S be a function of θ_5 , denoted as $US = S(\theta_5)$. Let the user battery-swapping consent rate P_1 be a function of θ_5 , denoted as $P_1 = P_1(\theta_5)$. The number of consenting users is $N_6(\theta_5)$, which is the product of the user set size and the user consent rate. The ultimate objective is to find the value of θ_5 that maximizes $N_6(\theta_5)$, expressed as:

$$N(\theta_5) = S(\theta_5) \cdot P_1(\theta_5) \quad (4)$$

2.5 Push Quantity Model for Vehicles

The operation capacity of the station is limited, so the number of pushed vehicles should not be excessive; otherwise, it will cause congestion and waste of resources:

$$N_t \leq \frac{t_h n_1}{t_c} \quad (5)$$

n_1 denotes the number of battery swap stations of the same brand within the power outage area, t_h is the duration of one push cycle, and t_c is the battery swapping time (including vehicle entry and exit).

2.6 Judgment Conditions for Valid Vehicles

$$C_2 \geq kQ_e \quad (6)$$

In the formula, C_2 is the real-time state of charge of the electric vehicle, which shall be no less than the minimum required power kQ_e of the battery to be swapped.

2.7 Information Push Strategy

2.7.1 Push Scheme Selection

Scheme A: Time Priority, Distance SecondaryFirst, take the shortest travel time as the screening criterion to obtain the time-optimal path set P_a (multiple paths may have the same travel time). From P_a , select the path with the shortest distance, which determines the final vehicle to receive push information.

Scheme B: Distance Priority, Time SecondaryFirst, take the shortest travel distance as the screening criterion to obtain the distance-optimal path set P_b . From P_b , select the path with the shortest time, which determines the final vehicle to be pushed.

Push Strategy: E is the real-time power of the battery swap station, E_{low} is the low-power alarm threshold, and E_{high} is the safe power level. When $E < E_{low}$, the swap station needs to replenish power as soon as possible and requires vehicles to arrive promptly. In this case, Scheme A is adopted. When $E > E_{high}$, the station power has reached the alarm threshold but not yet the safe level. To avoid energy waste and minimize travel consumption, Scheme B is adopted.

2.7.2 Solve for the shortest time

Calculate the actual speed of the j -th road segment on the i -th path:

$$v_{i,j}^{act} = v_{i,j}^{lim} \cdot c_{i,j} \quad (7)$$

$v_{i,j}^{act}$: actual driving speed of the j -th road segment on the i -th path. $v_{i,j}^{lim}$: legal speed limit of the j -th road segment on the i -th path. $c_{i,j}$: congestion coefficient of the j -th road segment on the i -th path.

The actual travel time of the j -th road segment on the i -th path is:

$$t_{i,j} = \frac{d_{i,j}}{v_{i,j}^{act}} = \frac{d_{i,j}}{v_{i,j}^{lim} \cdot c_{i,j} + \epsilon} \quad (8)$$

$d_{i,j}$ is the distance of the j -th road segment on the i -th path; $\epsilon=0.01$ is used to avoid division by zero.

The total actual travel time of the i -th path (sum of travel times of all road segments) is:

$$T_i = \sum_{j=1}^{m_i} t_{i,j} = \sum_{j=1}^{m_i} \frac{d_{i,j}}{v_{i,j}^{lim} \cdot c_{i,j} + \epsilon} \quad (9)$$

m_i is the number of road segments included in the i -th path.

Time minimization is expressed as follows:

$$\min Z_1 = \sum_{i=1}^{n_3} T_i \cdot x_p = \sum_{i=1}^{n_3} \left(\sum_{j=1}^{m_i} \frac{d_{i,j}}{v_{i,j}^{lim} \cdot c_{i,j} + \epsilon} \right) \cdot x_p \quad (10)$$

n_3 is the total number of alternative paths, x_p is the path selection variable, which equals 1 if the path is selected and 0 otherwise.

2.7.3 Solve for the shortest distance

Distance minimization is expressed as follows:

$$\min Z_2 = \sum_{i=1}^{n_3} \left(\sum_{j=1}^{m_i} d_{i,j} \right) \cdot x_p \quad (11)$$

2.8 Comparative Experimental Design

As shown in Table 1, the experiment is divided into three groups. In the experimental group, the number of pushed vehicles is set to the maximum value calculated according to the operating capacity of the battery swap station. With the push strategy applied, the real-time power values of the battery swap station within a specific time range are recorded. Since the operating capacity of the battery swap station has an upper limit, pushing an excessive number of vehicles is practically meaningless. Control Group 1 uses a relatively small number of pushed vehicles for comparison with the experimental group. Experimental Group 2 adopts the push strategy and only selects the nearest vehicles for pushing.

Table 1: Comparative test table

| Experimental group | Reasonable number of pushed vehicles | using push priority strategy |
|--------------------|--------------------------------------|------------------------------|
| Control group 1 | Lower number of pushed vehicles | using push priority strategy |
| Control group 2 | Reasonable number of pushed vehicles | nearest-vehicle push only |

3. Simulation

3.1 Solve for the Battery Level Value Returned to the User

θ_5 minimum battery level shall be determined to prevent resource waste caused by a threshold far exceeding the power required for the user's return trip, or inconvenience to the vehicle owner due to an excessively low threshold.

3.1.1 $N(\theta_5)$ critical value

To find the maximum value of $N(\theta_5)$, take the first derivative of $N(\theta_5)$ with respect to θ_5 : $N'(\theta_5) = S'(\theta_5)P_1(\theta_5) + S(\theta_5)P_1'(\theta_5)$. Set $N'(\theta_5) = 0$, at which an extreme point exists, $S'(\theta_5)P_1(\theta_5) + S(\theta_5)P_1'(\theta_5) = 0$.

To confirm that this critical point is a maximum, take the second derivative of $N(\theta_5)$: $N''(\theta_5) = S''(\theta_5)P_1(\theta_5) + 2S'(\theta_5)P_1'(\theta_5) + S(\theta_5)P_1''(\theta_5)$. Since $S'(\theta_5) < 0$ and $P_1'(\theta_5) > 0$, and in practical scenarios, the decreasing rate of the user set and the increasing rate of the user consent rate generally do not exhibit sharp opposing changes, it follows that $N''(\theta_5) < 0$, indicating that this critical point is a maximum point.

3.1.2 Determine the specific function

1) Simulation Data

In the simulation experiment, concentric circles are created, where circles with different radii represent different reachable ranges corresponding to the return battery level. Generally, electric vehicles trigger a low-battery alert when the remaining battery level is around 15%–20%. In this simulation, 20% is taken as the minimum return battery level provided to the user. Since most electric vehicles on the market have a battery capacity of 100 kWh, 20 kWh is set as the minimum value for θ_5 . The circle with radius R_1 represents the reachable range when the return battery level $\theta_5=20$ kWh.

The maximum value of θ_5 is set to avoid the range anxiety risk of low battery levels (below 20%) while not needing to reach a full charge (100%). Therefore, a median value of 50 kWh is chosen. A total of 16 concentric circles are constructed with radii R_1, R_2, \dots, R_{16} respectively. The circle with radius R_1 represents the reachable range at $\theta_5=20$ kWh, R_2 represents the range at $\theta_5=22$ kWh, and so on, with R_{16} representing the range at $\theta_5=50$ kWh.

1, 000 points are randomly distributed within the circles to represent the intended return positions of 1, 000 vehicles, as illustrated in Figure 1.

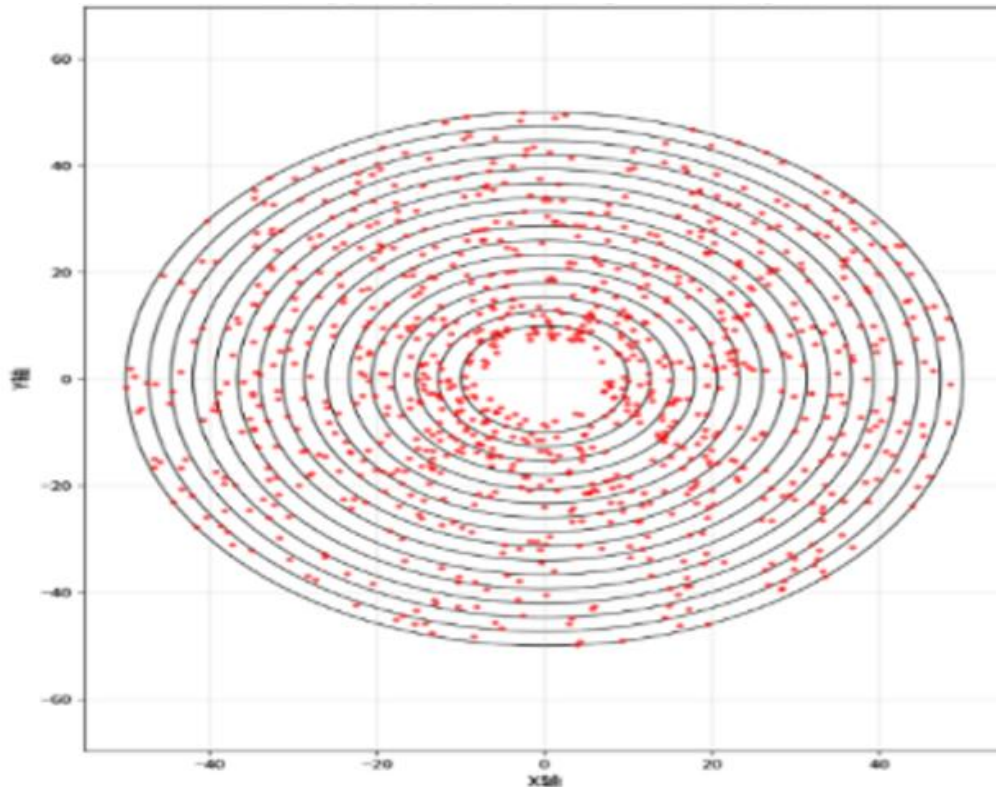


Figure 1: Vehicle return point simulation chart

Generally, electric vehicles trigger a low-battery alert when the remaining battery level is around 15%–20%. Given that the current rated battery capacity is 100 kWh, 1000 random integers between 15 and 100 are generated to represent the real-time battery levels of 1000 vehicles at a certain moment. For the convenience of calculation, it is assumed that the power consumption for vehicles to reach the battery swap station is zero, and the battery power exchanged to the station is 0. Thus, the battery power for all vehicles to return from the battery swap station is equal to their real-time battery level. We count the number of these 1000 random battery values that

are above 20, above 22, and so on up to above 50, which represents the number of valid users (S) meeting the battery requirement. Then we count the number of vehicles within different radii, which represents the number of reachable destinations, the number of users (P_1) who agree to the battery swap request. We record the P_1 and S values corresponding to $\theta_5=22, 24, 26, \dots, 50$ respectively. As shown in Table 2, as the return battery level increases, the number of users agreeing to the battery swap increases, while the number of users meeting the battery requirement decreases. The simulation results are consistent with practical requirements.

Table 2: Statistics table of power-qualified users and vehicle count capable of returning to destination

| θ_5 | 20 | 22 | 24 | 26 | 28 | 30 | 32 | 34 | 36 | 38 | 40 | 42 | 44 | 46 | 48 | 50 |
|------------|-----|-----|-----|-----|-----|-----|-----|-----|-----|-----|-----|-----|-----|-----|-----|------|
| P_1 | 88 | 139 | 203 | 272 | 341 | 389 | 472 | 518 | 571 | 649 | 706 | 785 | 848 | 900 | 944 | 1000 |
| S | 912 | 888 | 867 | 847 | 823 | 797 | 770 | 747 | 728 | 696 | 672 | 649 | 628 | 611 | 578 | 551 |

2) Function Selection

Candidate Functions for $S(\theta_5)$ (User Set Size):

a) Logarithmic function: $S(\theta_5) = a - b \cdot \ln(\theta_5 + c)$ ($a, b, c > 0$).

b) Power function: $S(\theta_5) = a \cdot \theta_5^{-b} + c$ ($a, b, c > 0$).

c) Exponential function: $S(\theta_5) = a \cdot e^{-b \cdot \theta_5} + c$ ($a, b, c > 0$).

Constraints: All functions must satisfy the actual data range "when $\theta_5 \in [20, 50]$, $S \in [551, 912]$ " to avoid negative values or fitting results beyond the reasonable interval. For the logarithmic function, $c > 0$ must hold to prevent $\theta_5 + c$ from being non-positive (which is meaningless). For the power function, b must be in the range $[0, 1]$ to ensure the decreasing rate aligns with reality.

Candidate Functions for $P_1(\theta_5)$ (User Agreement Rate):

a) Sigmoid function: $P_1(\theta_5) = \frac{d}{1 + e^{-k(\theta_5 - m)}}$ ($d, k > 0$, m is the inflection point)

b) Power function: $P_1(\theta_5) = a \cdot \theta_5^b + c$ ($a, b, c > 0$)

Constraints:

For the Sigmoid function, d should be close to 1000 (the maximum value of P_1) to avoid large deviations between the saturation value and the actual data.

All functions must satisfy the range "when $\theta_5 \in [20, 50]$, $P_1 \in [88, 1000]$ ", and the fitted value of P_1 should be close to 1000 when $\theta_5 = 50$.

3) Evaluation Criteria

Fitting Accuracy: Mean Squared Error (MSE): $MSE = \frac{1}{n} \sum_{i=1}^n (y_{\text{actual}} - y_{\text{fitted}})^2$, A smaller value indicates higher fitting accuracy;

Explanatory Power: Coefficient of Determination (R^2): $R^2 = 1 - \frac{\sum (y_{\text{actual}} - y_{\text{fitted}})^2}{\sum (y_{\text{actual}} - \bar{y})^2}$, The closer R^2 is to 1, the stronger the function's explanatory power for the variation in the data;

4) Performance Comparison

Comparison of Selected Functions for $S(\theta_5)$:

Logarithmic function: Parameters: $a=1052.36$, $b=189.24$, $c=8.72$ Performance: $MSE=12.87$, $R^2=0.9992$

Power function: Parameters: $a=1.2 \times 10^5$, $b=0.82$, $c=480$ Performance: $MSE=28.53$, $R^2=0.981$

Exponential decay function: Parameters: $a=850$, $b=0.02$, $c=520$ Performance: $MSE=42.15$, $R^2=0.968$

Comparison of Selected Functions for $P_1(\theta_5)$:

Sigmoid function: Parameters: $d=998.71$, $k=0.18$, $m=35.26$ Performance: $MSE=21.53$, $R^2=0.988$

Power function: Parameters: $a=0.03$, $b=2.5$, $c=50$ Performance: $MSE=35.72$, $R^2=0.975$

Conclusion:

The logarithmic function and the Sigmoid function form the optimal function combination, as they satisfy the requirement of "high fitting accuracy" ($MSE < 25$, $R^2 > 0.98$).

$$S(\theta_5) = 1052.36 - 189.24 \ln(\theta_5 + 8.72)$$

$$P_1(\theta_5) = \frac{998.71}{1 + e^{-0.18(\theta_5 - 35.26)}}$$

3.1.3 Objective Function Calculation

The Newton-Raphson iterative method is adopted, and derivative calculation and iterative convergence are implemented via MATLAB programming. The iteration interval is $\theta_5 \in [20, 50]$ (valid range), the initial value is $\theta_5^{(0)} = 35$ (the inflection point of the Sigmoid function, close to the optimal interval), and the convergence threshold is $|\theta_5^{(t+1)} - \theta_5^{(t)}| < 10^{-6}$.

The iterative formula is: $\theta_5^{(t+1)} = \theta_5^{(t)} - \frac{f(\theta_5^{(t)})}{f'(\theta_5^{(t)})}$. At the 7th iteration, $|\theta_5^{(7)} - \theta_5^{(6)}| = 2.2 \times 10^{-7} < 10^{-6}$, and the iteration converges to $\theta_5 = 37.03$.

Maximum Verification: $N''(\theta_5) = S''(\theta_5)P_1(\theta_5) + 2S'(\theta_5)P_1'(\theta_5) + S(\theta_5)P_1''(\theta_5)$, $N''(37.03) = -12.36 < 0$, confirming that $\theta_5 = 37.03$ is the maximum point.

3.2 Push Distance Calculation

According to industry data, the typical battery capacity of electric vehicles is currently $Q_e = 100\text{KWH}$, and the power consumption per 100 kilometers is $W_3 = 15\text{KWH}$. Based on the results of the practical case in the previous section, the hourly electricity consumption of the community corresponding to a battery swap station is $W_4 = 33\text{KWH}$, and the maximum capacity of a single battery swap station is 12 vehicles per hour.

Then, $\theta_4 \geq \frac{W_4}{N_t}$. Taking the minimum value, we have $33/12=2.75$ kWh. Thus, $Q_f = \theta_4 + \theta_5 = 39.75$ kWh, The push distance is calculated as: $S_2 = \frac{(Q_e - Q_f)}{w_3}$, the values yields $S_2 = 4$ km.

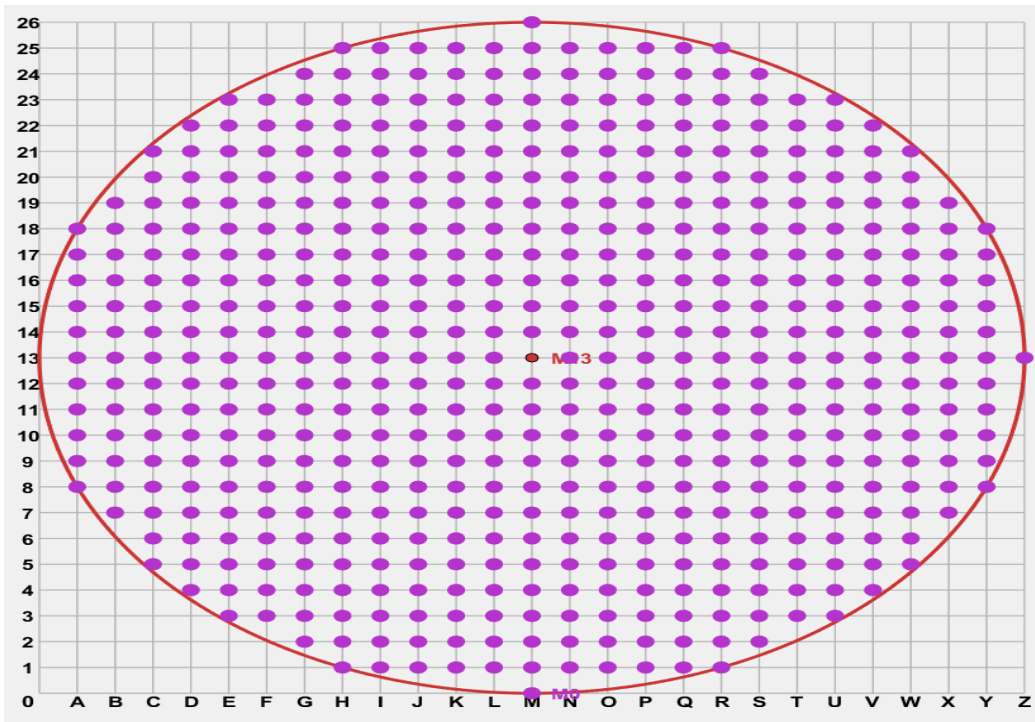


Figure 2: Road grid map

3.3 Simulated Push Strategy

3.3.1 Virtual Road Network Design

The maximum straight-line push distance is 4 km, so a circle with a radius of 4 km is established in the coordinate system as the pushable range. According to official data from Shanghai, there is an average of one traffic light every 300 meters on major roads in Shanghai. Calculating $8000/300 \approx 26$, the coordinate system is set to 26 grids, with each grid representing 0.3 km, as illustrated in Figure 2.

3.3.2 Data Preparation

Each coordinate in Figure 2 represents an intersection. We select 411 purple points in the figure and assume one vehicle is located at each intersection. Within the circle, there are 374 horizontal adjacent short segments and 374 vertical adjacent short segments, totaling 748 segments, which represent 748 road links. All factors affecting path selection, such as congestion and traffic lights, are unified into speed limits. According to research, the actual driving speed on non-highway urban roads in Shanghai ranges from 20 to 60 km/h. A speed limit is randomly generated for each segment within this range to represent random road conditions. The alarm and target values are determined based on the actual community electricity consumption and the total battery storage of the battery swap station. According to the practical case in Chapter 3, the emergency electricity supply required for residents at each station per hour is calculated as 33 kWh. A single push information cycle is set to one hour. To prevent the battery swap station from running too low on power, two hours of electricity are reserved, so the preset alarm value is $E_{low} = 66$ kWh. The total fully charged battery capacity of a single battery swap station is 1040 kWh, and 80% of this total is taken as the target value, so $E_{high} = 832$ kWh.

Logic of the experimental group push strategy: First, based on the real-time battery level, real-time road conditions, and

travel energy consumption of vehicles at each coordinate point, candidate vehicles are selected whose remaining battery power upon arriving at the battery swap station is greater than $kQ_e = \theta_4 + \theta_5 = 39.75$ kWh. When the total battery level of the swap station falls below the LOW threshold, Plan A (arrival time priority) is adopted: vehicles that can reach the swap station in the shortest time are selected first. If arrival times are tied, distance is prioritized. Ultimately, 12 vehicles are selected. The electricity supplied to the swap station by each of these 12 vehicles is calculated as their battery level at the time of push notification minus the travel energy consumption and the return trip energy consumption. The total battery level of the swap station is then computed from the electricity received within one hour and the community's hourly electricity consumption. Similarly, when the swap station's battery level reaches the HIGH threshold, the strategy switches to Plan B (distance priority): vehicles are selected by distance first, and if distances are tied, arrival time is prioritized. The hourly battery level of the swap station under Plan B is calculated accordingly.

Control Group 1 Push Logic: The strategy remains unchanged, and only 3 vehicles are pushed each time.

Control Group 2 Push Logic: 12 vehicles are pushed each time, but no strategy is applied—only the 12 closest vehicles are selected.

Conflict Filtering: Vehicles with arrival time conflicts are filtered out. Each battery swap process takes 5 minutes; vehicles arriving within the 5-minute window while the previous vehicle is swapping are excluded. If multiple vehicles arrive simultaneously, the one with higher battery level is selected.

Simulation via Python: The simulation was implemented using Python. As shown in Figure 3, the battery swap station in the experimental group started with the alarm-level battery

capacity E_{low} and adopted Plan A for vehicle push. The battery level rose steadily until it reached the target value E_{high} , at which point it switched to Plan B, stabilizing and fluctuating around the target value. The experimental group's strategy not only ensures continuous power supply to the residential community but also gradually recharges the battery swap station to the safe target value, enabling it to respond to more emergencies. Control Group 1: Due to the insufficient number of pushed vehicles, the battery level of the swap station remained below the alarm threshold and even showed a downward trend, making long-term continuous power supply impossible. Control Group 2: Without a scheduling strategy and only using a proximity-based push rule, the hourly battery level was highly unstable, posing a risk of power outage. The three groups of experiments met the expected objectives, clearly demonstrating the superiority of the scheduling strategy adopted in the experimental group.

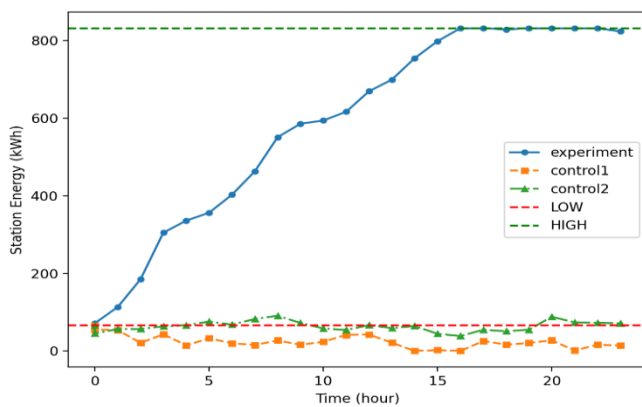


Figure 3: Power map of battery swapping station

4. Conclusions

Based on information network technology, this paper clarifies the online push range and quantity of battery swap information, establishes an optimization model for the user's safe return battery threshold, and proposes a dual-scheme strategy (Scheme A and Scheme B) combining online geographic information and real-time traffic data — prioritizing arrival time and distance respectively—to realize the online intelligent scheduling of emergency power supply resources for vehicle battery swap stations. Simulation comparison experiments based on the informatization characteristics of Shanghai's road network show that this online scheduling model can steadily raise the battery level of the swap station to the target value, significantly enhance the continuity and stability of emergency power supply, and effectively solve the problems of information lag and low resource allocation efficiency in the traditional offline scheduling mode. This study deeply integrates information network technology with the emergency power supply scheduling of battery swap stations, providing theoretical support and engineering reference for enhancing the grid's emergency resilience through digital technology and realizing the intelligent scheduling of emergency resources for vehicle battery swap stations. Future research can further combine big data and artificial intelligence technologies to optimize the user profile and online push algorithm of the information platform, improving the accuracy and efficiency of emergency scheduling for battery swap stations.

Acknowledgement

The work is supported by Innovation Fund Project for Undergraduate Student in Shanghai (No. SH2025080).

References

- [1] Palmer C. Battery Swapping Emerges as Major Alternative to Charging Electric Vehicles [J]. *Engineering*, 2025, 52(09): 6-9.
- [2] Jiang Lina. Design of Intelligent Vehicle Information Management System Based on Internet of Things [J]. *Special Purpose Vehicle*, 2024, (12): 106-108. DOI: 10.19999/j.cnki.1004-0226.2024.12.029.
- [3] Xu Xiangfeng, He Yalin. Research on Electric Vehicle Information Sharing and Intelligent Charging Platform Under the "Double Carbon" Goal [J]. *Automobile Applied Technology*, 2023, 48(23): 189-194. DOI: 10.16638/j.cnki.1671-7988.2023.023.035.
- [4] Zhang Meifang, Yue Hongfen. Research on Information Security Testing of Intelligent Connected Vehicles [J]. *Automotive Industry Research*, 2025, (01): 10-13.
- [5] He Shan, Chen Jiahao, Tang Wenjun, et al. Online Monitoring and Early Warning of Electric Vehicle Battery Health Status [J]. *Modern Automobile*, 2024, (15): 136-138.
- [6] Zhang Qiuyan, Gao Ping'an, Guo Hongxia, et al. Joint Online Monitoring of SOC and SOH for Electric Vehicle Lithium Batteries [J]. *Internet of Things Technology*, 2025, 15(04): 48-51. DOI: 10.16667/j.isnn.2095-1302.2025.04.012.
- [7] B M K, N A, S N K, et al. Optimizing battery health monitoring in electric vehicles using interpretable CART-GX model [J/OL]. *Results in Engineering*, 2025, 27: 106043. DOI: 10.1016/j.rinen-g.2025.106043.
- [8] RAMSHANKAR S, MANIMOZHI M. Integration of digital twin technologies for state estimation in electric vehicle batteries: A review [J/OL]. *Results in Engineering*, 2025, 27: 106858. DOI: 10.1016/j.rineng.2025.106858.
- [9] Hu Baoyu, Zhang Hengwei. Optimization of Scheduling for Electric City Buses in Cold Regions Based on Battery-Vehicle Matching [J/OL]. *Journal of South China University of Technology (Natural Science Edition)*, 1-13 [2025-12-27]. <https://link.cnki.net/urlid/44.1251.T.20251118.1138.003>.
- [10] Wang Wei, Liu Yixin. Research and Application of Intelligent Scheduling of Emergency Resources in Urban Expressway Network [J]. *Traffic & Transportation*, 2025, 41(05): 79-83.
- [11] Ji Mingquan. Technical Application of Vehicle Scheduling Automation and Visualization Based on Software Platform [J]. *Logistics Engineering and Management*, 2025, 47(06): 87-89+105.
- [12] TIWARI S, NASSIR N, LAVIERI P S. Ride-hailing vehicle dispatching and matching strategies to prioritize and complement public transport use [J/OL]. *Journal of Traffic and Transportation Engineering (English Edition)*, 2025, 12(5): 1484-1507. DOI: 10.1016/j.jtte.2024.09.010.
- [13] PENG F, WU W, LI D, et al. Charging dispatching strategy for electric vehicles considering willingness and status quo bias [J/OL]. *International Journal of*

Electrical Power & Energy Systems, 2025, 171: 111054.
DOI: 10.1016/j.ijepes.2025.111054.

- [14] Wei Guangyan. Research on Distributed Flexible Service Resources and Job Scheduling Based on Shared Manufacturing [D]. Shanghai University of Technology, 2024. DOI: 10.27308/d.cnki.gslgu.2024.000015.